25th ABCM International Congress of Mechanical Engineering
October 20-25, 2019, Uberlândia, MG, Brazil

COB-2019-0601
ANALYSIS OF FLUIDIZATION IN THE SPOUTED BED IN 3D VIA CFD FOR COFFEE GRAINS

Ana Paula Silva Artur[1]
[1]Chemical Engineer, Federal University of São João del Rei – UFSJ - Campus Alto Paraopeba
e-mail: anaps.artur@gmail.com

Elaine Cristina Batista da Silva[2]
[2]Chemical Engineer, Federal University of São João del Rei – UFSJ - Campus Alto Paraopeba
e-mail: ellainecristinaa@hotmail.com

Tuane Tayrine Mendes Cardozo[3]
[3]Chemical Engineer, Federal University of São João del Rei – UFSJ - Campus Alto Paraopeba
e-mail: tuanetayrine@hotmail.com

Welberth Santos Laizo[4]
[4]Chemical Engineer, Federal University of São João del Rei – UFSJ - Campus Alto Paraopeba
e-mail: welbs@msn.com

Reimar de Oliveira Lourenço[5]
[5]Teacher of Federal University of São João del Rei – UFSJ - Campus Alto Paraopeba
e-mail: reimar@ufsj.edu.br

Abstract. *The spouted bed can be used in several industrial operations due to the efficient fluid-particle contact and the high rates of mass and heat transfer, among then we can mention the drying of grains and pastes and the granulation of materials. However, this equipment still has scale-up restrictions, which restricts its use to small-scale and meso-scale processes. One way to study equipment operating behavior at lower costs is to use computational tools to verify and analyze the best performance of this equipment for a requested operation. The objective of the study was to verify the fluid dynamics behavior of a conventional bed of solid gas type in bench scale for coffe through CFD simulation (Computational Fluid Dynamics). The simulations presented in this article show a dynamic flow profile inside the bed.*

Keywords: *Spouted bed; CFD; Flow dinamics profile*

1. INTRODUCTION

According to (Grissom; Loeb and Mitani, 2011) the spouted bed was obtainded by a modification in a fluid bed, as developed by Mathur and Gishler (1995), they noted that this type of bed is effective for processes of contact between gas and particles. Grissom, Loeb and Mitani, (2011) reports that the spouted bed has particular characteristics that allow it to perform operations that require more homogeneous cyclic movement of the particles, which can not be performed in a fluidized bed.

The spouted bed has numerous possibilities of use, mainly to its excellent fluid-particle contact, which makes it an advantage over equipment that operates in a fixed bed (Araújo and Santos, 2015). Its original cone-cylindrical form, called conventional, can present some modifications that aims the best use of this equipment according to a request for use (Chatterjee, 1970). However, the conical base of the spouted bed is used to increase the movement of solids and to eliminate dead spaces at the bottom of the bed (Duarte et al., 2015).

The possibility of application of the spouted bed has increased because it combines advantages like the effectiveness in treating physico-chemical transformations, or even reactions that involve simultaneously heat and mass transfer in combination with particles of different sizes. These procedures are important in heating operations such as drying, pyrolysis, combustion (Link et al. (2005); Sutkar; Deen and Kuipers, 2013). In spite of the many advantages, the springs still have some limitations to the operation and the control, as well as the instability of the spurt (Sutkar; Deen and Kuipers, 2013).

According to Artur et al., (2018) and HosseinI; Zivdar and Rahimi, (2009) Computational Fluid Dynamics (CFD) technique has been used as a numerical tool in the modeling of multiphase flows, allowing analysis and understanding of the flow behavior of multiphase systems, promoting cost and disign time reductions.

CFD models can be divided into two groups, Lagrangian and Eulerian. In Lagrangian models, or discrete particle models (DPM), the two-dimensional motion of each individual particle is calculated directly from the forces acting on them, being responsible for the interaction between the particle and the gas phase. In the multifluid CFD model, also referred to as Eulerian - Eulerian (EE), the gaseous and solid phases are considered continuous and fully interpenetrating. Both phases are described in terms of separate sets of conservation equations with appropriate interaction terms representing the coupling between the phases (Duarte; Murata and Barrozo, 2008).

According to Santos (2011) the Eulerian model is adequate when gravity is acting in a relevant way in the separation between the phases and due to this characteristic this Eulerian model is suitable for application in the spouted bed. Other equipments that present this same characteristic and uses this model are bubble columns, risers, particle suspension, fluidised beds, among others.

The satisfactory results of a project that makes use of Computational Fluid Dynamics, passes through the choice and adequate generation of the mesh, exactly for its importance this procedure consumes a greater time in the CFD analysis (Santos; Duarte and Júnior, 2010). The flexibility which the mesh will adapt to the system is inversely proportional to the precision, the greater the precision, the less flexibility of the system, therefore the refinement of the mesh must occur in the regions of interest, in this field the regions where the flow is predictable is not the center of the analyzed problem, for this reason a less refined mesh reduces the computational effort and improves precision (Artur et al., 2018).

This research aimed to verify, through CFD (Computational Fluid Dynamics) simulation, the fluid dynamics behavior of a conventional spouted bed of solid gas in bench scale type for the coffee grains, besides verifying that the mesh, model and the time increment adopted will provide satisfactory results.

2. MATERIALS AND METHODS

In this study, a conventional spouted bed with dimensions as described in Fig. 1 was used as the base. The simulation strategy adopted was the three-dimensional simulation (3D) of a commercial CFD package that uses the Finite Volume Method (FVM) for the numerical processing of the problem because to the available processing capacity. The FVM consists of dividing a control volume into several smaller control volumes until it reaches a dimension that makes the equations to be solved within this volume as a point function, iterating or simultaneously solving the whole set of differential equations obtained. This method makes the governing equations discretized within the computational domain (time space) (Blanco, 2013).

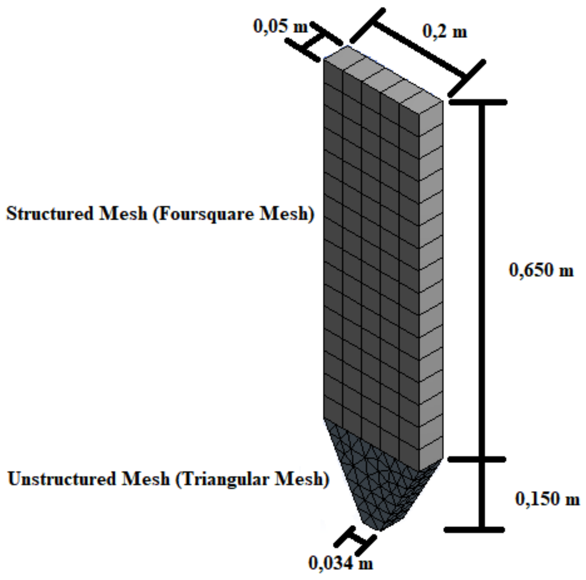

Figure 1. Quenched spouted bed and presentation of the hybrid mesh (Foursquare *Mesh* - 0.05 *mesh* and Triangular *Mesh*- 0.025 *mesh*).

In the present study, the organic material (coffee grain) was used, the characteristics of interest for the simulation of this material are shown in Tab. 1 (all data in the Tab. 1 that has units is in SI). In CFD simulation the mesh configuration used was unstructured (trigonal) in the conical base and structured mesh (square) in the body part, this configuration where the unstructured and structured mesh is used is called the hybrid mesh, this composition was chosen because it provides a gain in computational effort, improving the processing of the computer used. The Eulerian multiphase model was adopted, which treats gas and particles as an interpenetrating continuum. This numerical approach minimizes the computational cost, especially for flows with high particle concentration, and also considers the effects of the interaction between the two phases. As the volume of one phase can not be occupied by the other, the concept of phase volume fraction is introduced, in which in the project in question 40% air and 60% particulate were used. These volume fractions are assumed to be continuous functions of space and time. The laws of conservation of mass and momentum must be satisfied for each phase individually.

Table 1. Parameters and contour conditions used in the simulations for the grain of organic coffee material. Available from: (Guevara-Barreto; Castaño-Castrillón and Guevara, 2005);

COFFEE	
Model Eulerian Granular : (Implicit)	
Interaction fluid particle : Gidaspow	
Particule Granular	Diameter particule: 0.015 m
	Granular Viscosity: Gidaspow
	Granular Bulk Viscosity: Lun-et-al
	Pression solids: Symlal-Obrien
	Distribuicion radial: Lun-et-al
Condition in Inlet: Velocity Inlet	
Pressure reference to bed exit	
Parameters Relaxation	Pression: 0.2
	Density: 1
	Forces Body: 1
	TemperatureGranular : 0.2
	Momentum: 0.2
	Fraction Volumetric : 0.2
Maximum Iteration / Time Step	200
Criterion of Convergence of Waste	10^{-3}
Time Step	10^{-3} s

The conservation equations are written for both phases, which gives a system of similar equations, facilitating the mathematical manipulation of it. The proper description of the interfacial forces present in the momentum balance equations of both phases have fundamental importance in the accuracy of the simulations, with the drag force in Eq. (1) being the main force acting on the particles (Santos, 2011), the drag force corresponding to momentum transfer at the interface between the gaseous and solid phases is one of the dominant forces in momentum balances (Taghipour, Ellis and Wong, 2005). The drag force exerted on the particles in liquid-solid systems is shown below:

$$\overrightarrow{f}_{drag} = K_{fs}(\vec{v}_s - \vec{v}_f) \tag{1}$$

The drag model used between the gas phase and the granular phases was the model of Gidaspow et al. (1992), because for the spouted bed this model is the most appropriate due to the difference in particle concentration in the characteristic regions of this bed. The mathematical modeling of this system requires the application of the theory of granular flows, which will be informed ahead. This model consists of a combination of the Wen and Yu (1966) (for diluted phase) and the Ergun (1952) (for the dense phase). When $\alpha_f < 0{,}8$, the fluid-solid exchange coefficient K_{fs} is as Eq. (2).

$$K_{fs} = 150\frac{\alpha_s(1-\alpha_f)\mu_f}{\alpha_f d_s^2} + 1{,}75\frac{\rho_f \alpha_s |\vec{v}_s - \vec{v}_f|}{d_s} \tag{2}$$

Where:
μ_f: is the Fluid viscosity;
d_s are the phases particles diameters;
α_s e α_f are the volumetric fractions,
$|\vec{v}_s - \vec{v}_f|$ is the relative velocity between the phases

ρ_f is the phase density;

As informed by the approach of the Euler-Euler model, it considers the phases continuous and interpenetrating, so there are no voids or spaces and there is no space defined for each phase. The volumetric fraction α, quantifies each phase in the control volume and by definition the sum of the fractions is equal to one Eq. (3).

$$\alpha_s + \alpha_g = 1 \tag{3}$$

For the mass conservation caracterization is used the Eq. (4) and Eq. (5):

$$\frac{\partial}{\partial t}(\alpha_g \rho_g) + \nabla(\alpha_g \rho_g \vec{v}_g) = \sum_{p=1}^{n} \dot{m}_{pq} - \alpha_q \frac{d_q \rho_q}{dt} \tag{4}$$

$$\frac{\partial}{\partial t}(\alpha_s \rho_s) + \nabla(\alpha_s \rho_s \vec{v}_s) = \sum_{g=1}^{n}(\dot{m}_{fs} \dot{m}_{sf}) + S_s \tag{5}$$

Being $\dot{m}$ the mass transfer rate, S is the mass source term. Since the mass transfer between phases is not considered, the right side of Eq. (4) and (5) are zero.

The Eq. (6) momentum transport to the gas phase is:

$$\frac{\partial}{\partial t}(\alpha_f \rho_f \vec{v}_f) + \nabla(\alpha_f \rho_f \vec{v}_f \vec{v}_f) = -\alpha_f \nabla p + \nabla . \bar{\bar{\tau}}_f + \alpha_f \rho_f \vec{g} + \sum_{p=1}^{n}(\vec{K}_{fs}(\vec{v}_s - \vec{v}_f) - \dot{m}_{fs} \vec{v}_{fs}) + \\ + \alpha_f \rho_f (\vec{F}_f + \vec{F}_{lift,f} + \vec{F}_{vm,f}) \tag{6}$$

Where $\vec{g}$ is gravity, $\vec{F_f}$ it is the field force, $\vec{F}_{lift,f}$ it is the ascending force acting on the particle, mainly due to the velocity gradients in the primary phase flow field (f). This ascending force is the most significant for larger particles. The virtual mass force is represented by $\vec{F}_{vm,f}$ and the velocity at the interface is represented by $\vec{v}_{fs}$. The velocity at the interface is related to mass transfer, for example if there is mass transfer from the solid phase to the fluid phase then $\vec{v}_{fs} = \vec{v}_s$. However if there is mass transfer from the fluid phase to the solid phase then $\vec{v}_{fs} = \vec{v}_f$.

The Eq. (7) momentum transport to the solid phase is:

$$\frac{\partial}{\partial t}(\alpha_s \rho_s \vec{v}_s) + \nabla(\alpha_s \rho_s \vec{v}_s \vec{v}_s) = -\alpha_s \nabla p + \nabla . \bar{\bar{\tau}}_s + \alpha_s \rho_s \vec{g} + \sum_{p=1}^{n}(\vec{K}_{fs}(\vec{v}_s - \vec{v}_f) + \dot{m}_{fs} \vec{v}_{fs}) + \\ + \alpha_s \rho_s (\vec{F}_s + \vec{F}_{lift,s} + \vec{F}_{vm,s}) \tag{7}$$

To consider these effects, several empirical correlations were proposed to quantify the energy transmitted from the gas phase to the solid phase. Among the most used models in the modeling and simulation of fluidized beds are the models of (Gidaspow et al.,1992), the (Syamlal and O'Brien, 1989) and the (Wen and Yu, 1966). In this work the Gidaspow model was evaluated, since it was the model employed.

The goal of kinetic theory of granular flow is to represent the interactions between the particulate phase of a multiphase flow. It is based on the kinetic theory of dense gases, but the usual temperature is replaced by a granular temperature. The other properties of the solid phase, such as pressure and viscosity, are a function of this granular temperature (Hodapp, 2009). The granular temperature, θ_s, is defined for each solid phase, and is described as the specific kinetic energy of the velocity fluctuations of the particles Eq. (8):

$$E_{\theta_s} = \frac{3}{2}\theta_s \tag{8}$$

Where E_{θ_s} is the granular energy. The energy transport of the granular mixture can be solved and then the granular temperature for the solid phase can be obtained.

The Eq. (9) of transport derived from kinetic theory has the following form:

$$\frac{3}{2}\left[\frac{\partial}{\partial t}(\alpha_s \rho_s \theta_s) + \nabla(\alpha_s \rho_s \vec{v}_s \theta_s)\right] = \left(-p_s \bar{\bar{I}} + \bar{\bar{\tau}}_s\right) : \nabla \vec{v}_s + \nabla(k_{\theta_s} \nabla \theta_s) - \gamma_{\theta_s} + \phi_{fs} \tag{9}$$

Where:

- $\left(-p_s \bar{\bar{I}} + \bar{\bar{\tau}}_s\right) : \nabla \vec{v}_s$= power generation by tensor solids tension;

- $k_{\theta s}\nabla\theta_s$= diffusion of energy ($k_{\theta s}$ is the diffusion coefficient);
- $\gamma_{\theta s}$ = collisional energy dissipation;
- ϕ_{fs}= exchange of energy between fluid phase f and solid phase s.

3. RESULTS AND DISCUSSION

The results of the simulation are exhibited in the Fig. 3, it is possible to observe the behavior of the bed at each stage of its operation: the fixed bed, the established jet and the transition between them, as well as distinguish the three different characteristic regions of the jet bed: ring region, internal jet and fountain. It is also noted that as expected in the annular region the fraction of solids is higher than in the region of the internal jet.

With increasing velocity it is possible to note that the bed passes from the minimum sprue condition to the stable sprung condition. At the end of these simulations, it is expected to observe the characteristic regions of the spurt, as shown in the Fig. 2.

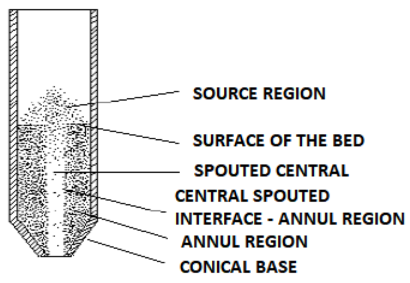

SPOUTED CENTRAL : Region of greater porosity in the bed where the pneumatic transport of the particles occurs with concurrent movement of the material;
SOURCE REGION: Region above the bed, where the particles coming from the central stream decelerate falling in the annul region.
ANNUL REGION - In this region the particles that fall from the source region slide, in part, to the base of the bed in a countercurrent motion with the air;
SURFACE OF THE BED: bed ridge to which the source region will surface after the spouted is established;
CENTRAL SPOUTED INTERFACE - ANNUL REGION: Imaginary frontier between the annular region and the spouted central. In this region, there are some problems such as "short circuits", which are nothing more than the premature migration of the solids from the annular region to the spouted central, thereby decreasing the residence time of the particle in the annular region, strongly affecting the homogeneity of the product.

Figure 2. Scheme of a spout bed. Available from: (Lourenço, 2006)

In the Fig. 3, the porosity profiles of the jet bed faces the conditions of simulation Tab. 1. In this way is possible to verify the influence of refining the mesh and the increment of time adopted in the quality of the results.

Volume Fraction	3D	Front View	3D	Front View	3D	Front View	3D	Front View	3D	Front View	3D	Front View	3D	Front View
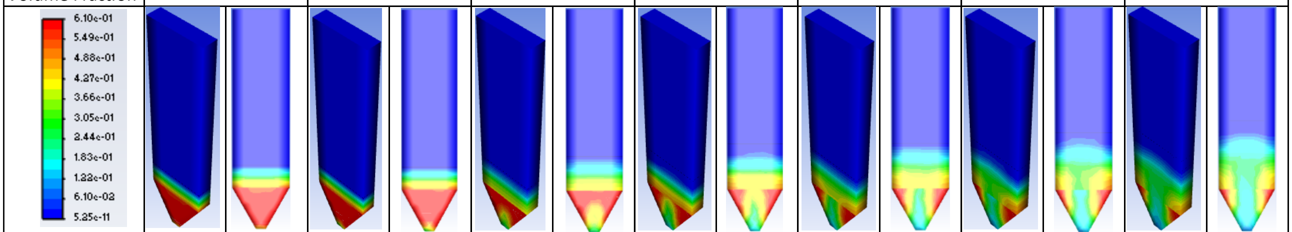														
	U = 1 to 4 m/s		U = 5 - 7m/s		U = 10 m/s		U = 15 m/s		U = 20 m/s		U = 25 m/s		U = 30 m/s	
	Fixed Bed		Internal Jet (Conical Base)		Minimum Spouted (Annul Region)		Transition from Minimum Spouted to Stable Spouted (Central Spouted Interface - Annul Region)		Stable Jorro - beginning Enlargement of the Preferential Channel (Spouted Central)		Stable Jorro - Expansion of the Preferential Channel (Surface of the bed)		Stable Jorro - Complete Formation of the Preferential Channel (Source Region)	

Figure 3. Profile of Spouted Bed Porosity for hybrid mesh for the grain of organic coffee material.

Initially, it was verified that with small air flows the fluid only percolated between the particles and the system behaved as a fixed bed (velocity of 1 to 4 m/s). With the increase of the air flow, it was noticed a high agitation of the particles in the bed base, characterizing the formation of an internal cavity due to the action of the air jet, enough to displace the particles. This cavity was gradually increased leading to a centered preferential channel, known as an internal jet (velocity of 5 to 7 m/s), which extended to the point of incipient spurt (minimum spurt), being imminent to appear on the surface of the bed. At the moment that the internal channel was ruptured, causing the formation of the spout on the surface of the bed (velocity of 25 m/s), leading to the expansion and providing the formation of the source region (velocity of 30 m/s). From this point forward, any increase in air flow only caused the increase of height of the source to rise and a slight decrease in the pressure drop.

The plots with the points of pressure drop of the system obtained in the time of 4 s was performed for the velocities of 0 to 30 m/s. These data are arranged in the Fig. 4, 5, 6 e 7**.** In this, the pressure drop plot obtained through the Average Area (Area), from where the data of Air Input (Input), Interior of the Reactor (Interior) and, finally, Average Volume (Volume) were obtained. In the first three plots the information is obtained through surface integrals and the last one by volume integrals.

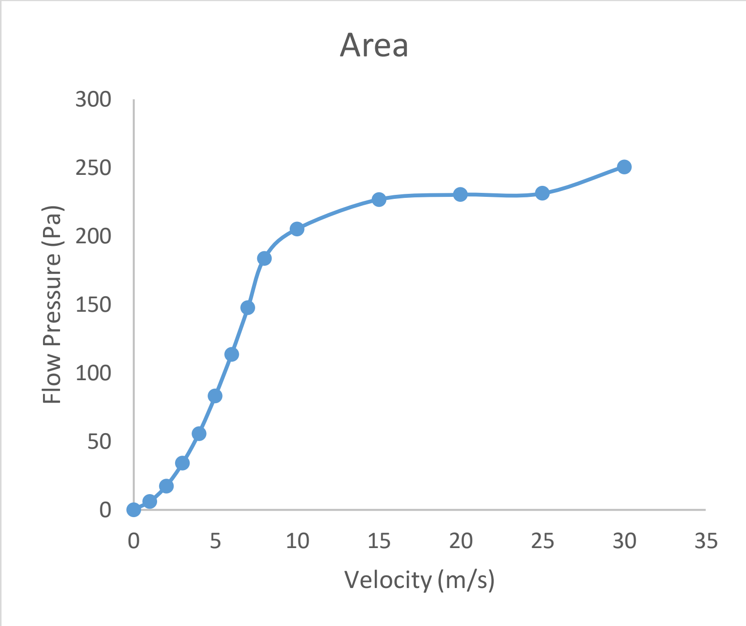

Figure 4. Plot of pressure drop versus air inlet velocity for the time of 4s, for Average Area.

From the plot shown in Fig. 4, it is noted that the value for pressure drop has a marked increase for the first velocities exactly in the fixed bed region up to the minimum spurt condition. From the minimum spurt transition to the stable spurt, a peak is formed and when entering the stable stream it closely look like constant which are the velocities of turbulence.

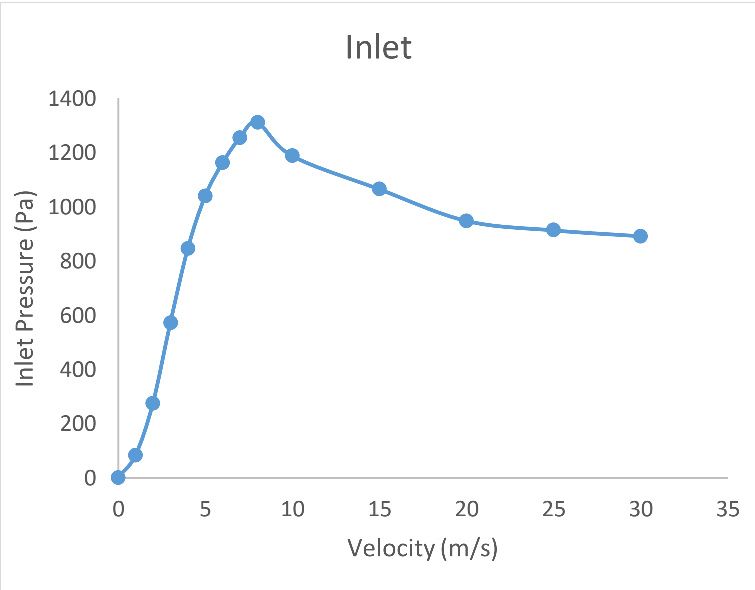

Figure 5. Plot of pressure drop vs. air inlet velocity for instant 4 s, for Air inlet.

The plot of Fig. 5 corresponds to the variation of the system pressure at the air inlet at the bed base, ensure that a linearity at the initial points, which is justified by the fact that this parameter was adopted as constant in the elaboration of the project. This curve corresponds to those found in literature, being similar to that expected for a spouted bed as indicated by Barcelos (2006) and Ferraz et al. (2017). Comparing the fluidization curve obtained with that obtained experimentally by Ferraz et al., (2017), it can be noticed that the regions presented in the curve are similar and the fluidization and transition velocities of the spout occurred at similar velocities. This variation is expected due to the difference between the solid materials used.

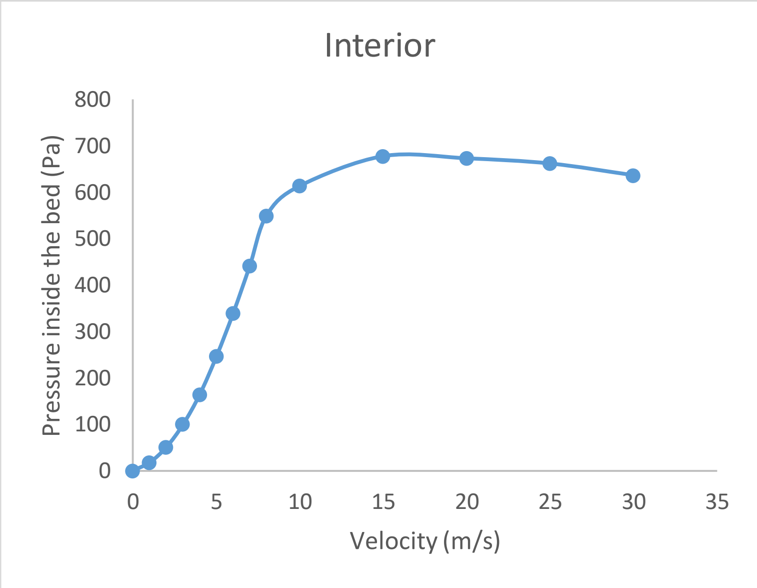

Figure 6. Plot of pressure drop vs. air inlet velocity for the instant of 4 s, for reactor interior.

From the visualization of the plot of Fig. 6, it is possible to observe that this one presents similarities with Fig. 5, since both represent floating moments of the process, this is more visible at the initial points where the bed was fixed and migrated to minimum spurt.

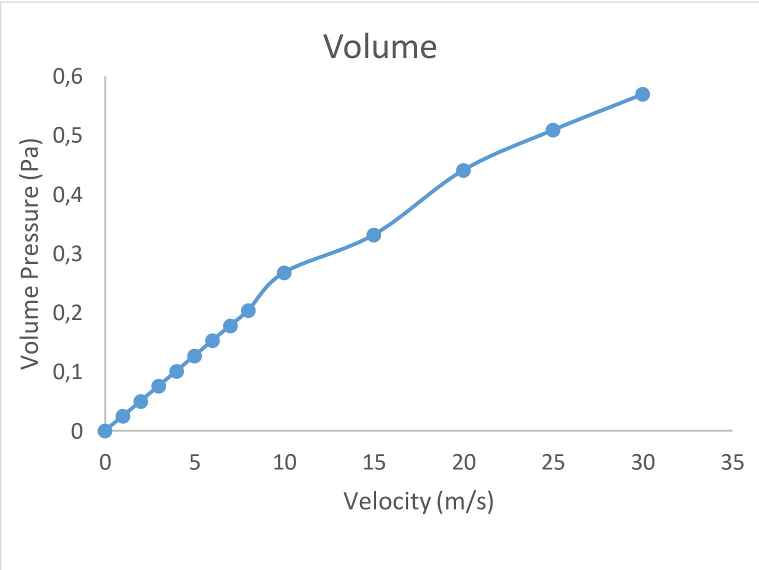

Figure 7. Plot of pressure drop versus air inlet velocity for the instants 4 s, for Average Volume.

On the other hand the plot of Fig. 7, shows a greater difference when compared to the previous ones, this is due to the same one being obtained by a different method, that is the method of volume integrals. The differences can be explained by the randomness applied to the calculations involved in the process.

From the analysis of Fig. 4 to 7 it is noticed that there is no great variation in the initial characteristics of the system, only when it is getting turbulent there is a great variation in the values of pressure drop, as seen from the point of velocity 15 m/s. It was expected due to the chaotic movement as a primary characteristic when the system takes the turbulent regime as a pattern of action, demonstrating that the point of minimum fluidization is close to this point. At this point there is a tendency of the system to maintain the condition for a range of air flow variation, making it important to present a parameter directly linked to the cost of the operation, since it is at this point that much of the process energy is consumed.

4. CONCLUSIONS

In the present study, it was evaluated whether the model of drag was satisfactory, observing if the model represents the flow pattern characteristic of the stream bed, identified by the distinction between the spurt, annular and source regions, checking if there was a good representativeness of the real system.

The time increment used in the simulation was 1.10^{-3} s, with this time increment used at high velocity, a high computational requirement was perceveid, due to the simulation being performed in the 3D model, as the results when evaluating the frames were already satisfactory, there was no need to decrease the time step for 1.10^{-4} s.

With the results obtained, the performance of the spurt can be improved since it not requires so much experimentation, because with this information the most adequate velocity for the formation of the source is known (place where the best efficiency of the equipment is being taken), consequently the time to establish the source in the sprue bed will be reduced, obtaining in a faster and efficient way to operation.

Finally, the porosity profile frames sh0o0wed0 the flow dynamics in the bed and it was observed that the establishment of the stable sprue occurred with a clear view of the characteristic source region, so the results found in this study are in agreement with those in the literature.

5. REFERENCES

Araújo, B. S. A., Santos, K. G. Dos., 2015. *Estudo dos regimes de escoamento do leito de jorro fluidizado com tubo draft empregando fluidodinâmica computacional*. Anais do XXXVII Congresso Brasileiro de Sistemas Particulados. Anais...São Paulo: Editora Edgard Blücher.

Artur, A. P. S., Silva, E. C. B. Da, Cardozo, T. T. M., Laizo, W. S., Lourenço, R. De O., 2018. "SIITA - Estudo Fluidinâmico do Leito de Jorro 2D". *Revista Higiene Alimentar*, v. 32, n. 0101–9171, pp. 111–116.

Bacelos, M.S., 2006. *Análise do comportamento da fluidodinâmica do leito de jorro com misturas de tamanho de partículas.* Doctoral Thesis in Chemical Engineering. Universidade Federal de São Carlos, pp. 113.

Chatterjee, A., 1970. "Spout-Fluid Bed Technique". *Industrial & Engineering Chemistry Process Design and Development*, v. 9, n. 2, pp. 340–341.

Duarte, C. R., Barroso, M. A. De S., Santos, D. A., Júnior, I. P., 2015. Estudo experimental e de simulação da fluidodinâmica de um leito de jorro operando em fase diluída. Universidade Federal de Uberlândia, Faculdade de Engenharia Química, Campus Santa Mônica – Uberlândia/MG. V. 9, Nº. 1, pp. 1–21.

Duarte, C. R., Murata, V. V., Barrozo, M. A. S., 2008. "Experimental and numerical study of spouted bed fluif dynamics". *Brazilian Journal of Chemical Engineering*, v. 25, n. 1, pp. 95–107.

Ferraz, H. P., Ferreira, J. H., Porto, F. R. B. D., Oliveira, A. B., 2017. *Estudo Da Fluidodinâmica Em Leito De Jorro E Fluidizado Com Partículas De Soja*. Anais do XII Congresso Brasileiro de Engenharia Química em Iniciação Científica. Anais...UFSCar – São Carlos – São Paulo.

Grissom, J., Loeb, S., MitanI, H., 2011. "Estudo experimental e de simulação da estabilidade fluidodinâmica do leito de jorro operando com mistura de partículas". v. 5, pp. 1–8.

Gidaspow, D., Bezburuah, R., Ding, J., 1992. "Hydrodynamics of circulating fluidized beds, kinetic theory approach in fluidization", In: *Proceedings of the 7th Engineering Foundation Conference on Fluidization*, pp. 75-82.

Guevara-Barreto, R. A.; Castaño-Castrillón, J.; GuevarA, R., 2005. Caracterización granulométrica del café colombiano tostado y molido**.** *Cenicafé.* v. 56, n. 1, pp. 5–18.

Hosseini, S. H., Zivdar, M., Rahimi, R., 2009. "CFD simulation of gas–solid flow in a spouted bed with a non-porous draft tube". *Chemical Engineering and Processing: Process Intensification*, v. 48, n. 11–12, pp. 1539–1548.

Hodapp, M . J., 2009. *Modelagem e Simulação de um Leito Fluidizado: Um Estudo Comparativo*. Masters Dissertation, Universidade Estadual de Campinas, pp. 113.

Link, J.M., Cuypers, L.A., Deen, N.G., Kuipers, J.A.M., 2005. "Flow regimes in a spout–fluid bed: A combined experimental and simulation study". *Chemical Engineering Science*, v. 60, n. 13, pp. 3425–3442.

Lourenço, R. De O., 2006. *Identificação e monitoramento de regimes de escoamento em leito de jorro*. Masters Dissertation. Universidade Federal de Uberlândia, pp. 133.

Lun, C. K. K., Savage, S. B., Jeffrey, D. J., Chepurniy, N., 1984. "Kinetic Theories for Granular Flow: Inelastic Particles in Couette Flow and Slightly Inelastic Particles in a General Flow Field, J. Fluid Mech.", v. 140, pp. 223–256.

Mathur, K. B., Gishler, P. E., 1955 "A technique for contacting gases with coarse solid particles". *AIChE Journal*, v. 1, n. 2, pp. 157–164.

Santos, D. A., Duarte, C. R., Júnior, I. P., 2010. "Caraterização experimental e de simulação dos regimes de estabilidade e influência da mistura de particulas na fluidodinâmica de um leito de jorro". V. 4, pp. 1–22.

Syamlal, M., O'Brien , T. J., 1989. "Computer simulation of bubbles in a fluidized bed". *AIChESymp. Series,* V. 85, pp. 22-31.

Sutkar, V. S., Deen, N. G., Kuipers, J. A. M., 2013. "Spout fluidized beds: Recent advances in experimental and numerical studies". *Chemical Engineering Science*, v. 86, pp. 124–136.

Taghipour, F., Ellis, N., Wong, C., 2005. "Experimental and computational study of gas–solid fluidized bed hydrodynamics". *Powder Technology*. V. 60, pp. 6857 –6867.

Wen, C. Y., Yu, Y. H., 1966. "Mechanics of fluidization, Chem". *Eng. Prog. Symp.Series*, V. 62, pp. 100-111.

6. RESPONSIBILITY NOTICE

The authors are the only responsible for the printed material included in this paper.